

Title: Elucidating multipollutant exposure across a complex metropolitan area by
systematic deployment of a mobile laboratory

Ilan Levy, Cristian Mihele, Gang Lu, Julie Narayan, Nathan Hilker and Jeffrey R. Brook

Supplemental Material

Table of Contents

A.	Supplemental Figures.....	2
B.	Supplemental Table	5
C.	Description of the instrumentation inlets to CRUISER:.....	6
D.	Speed correction for particulate matter (PM) measurements	8
E.	Comparison of CRUISER's and VdM measurements.....	13

A. Supplemental Figures

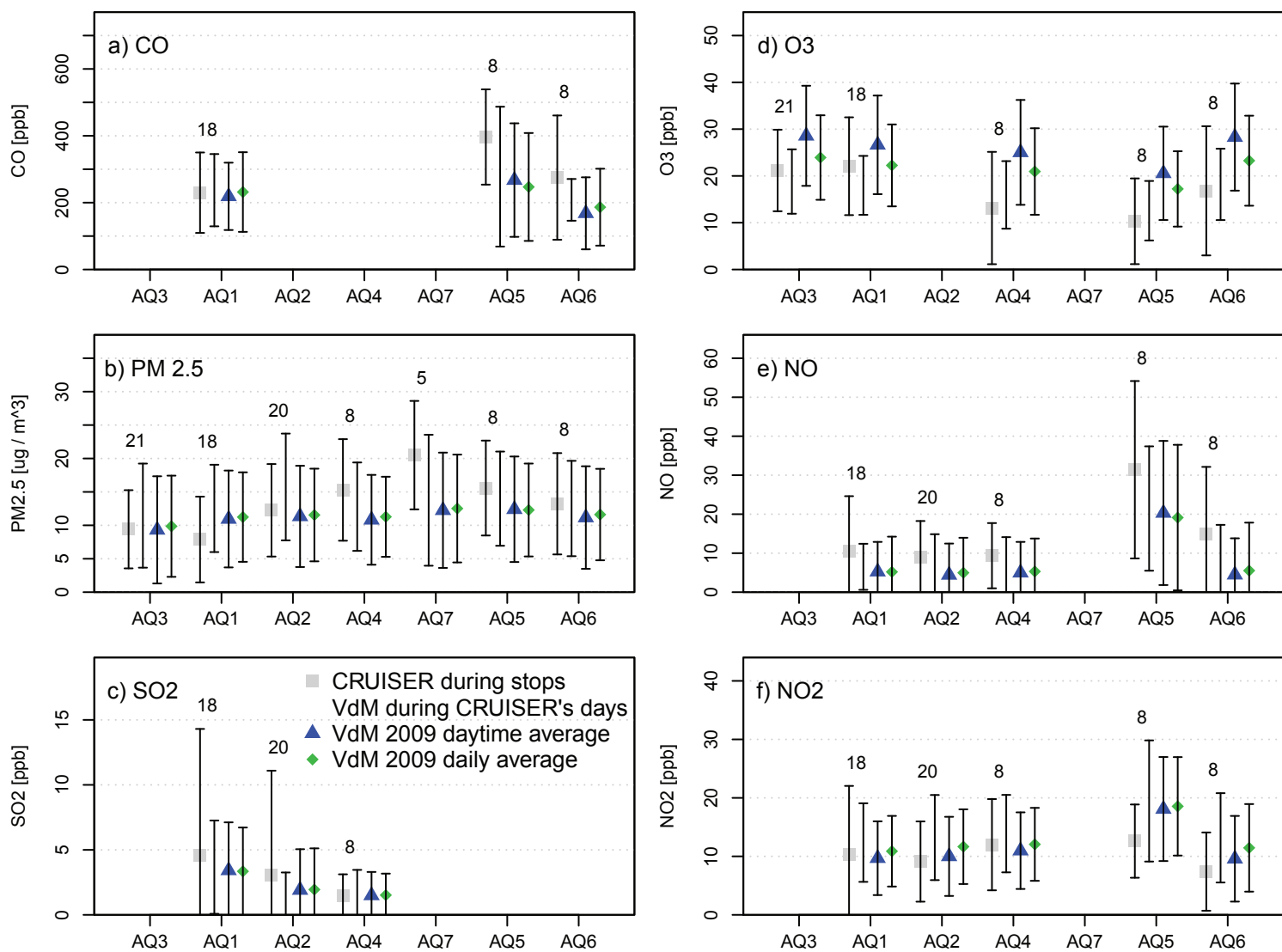


Fig. SM-A1: Same as Fig. 2 for CO (a), PM_{2.5} (b), SO₂ (c), O₃ (d), NO (e) and NO₂ (f).

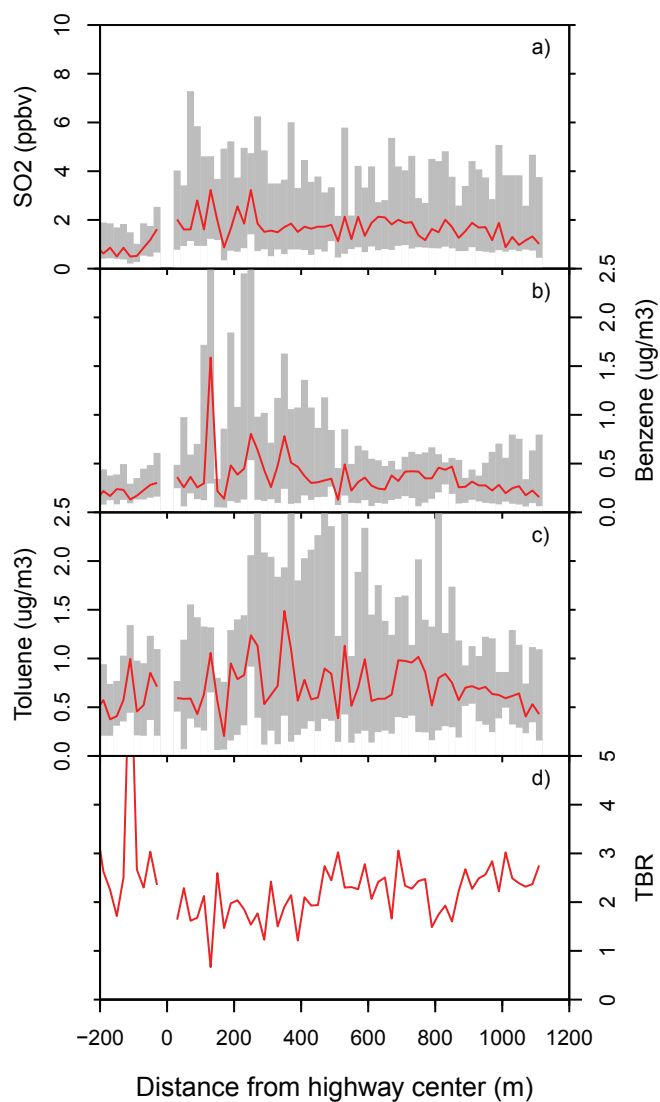


Fig. SM-A2: Median pollution levels (red) line and IQR (grey) at 20 m bins for the entire study for SO_2 (a), benzene (b) and toluene (c) along the cross section taken on Avenue Marien crossing Highway 40, location is marked in Fig. 3a. The toluene to benzene ratio (TBR) is shown in (d). Only bins with more than 7 measurements are plotted.

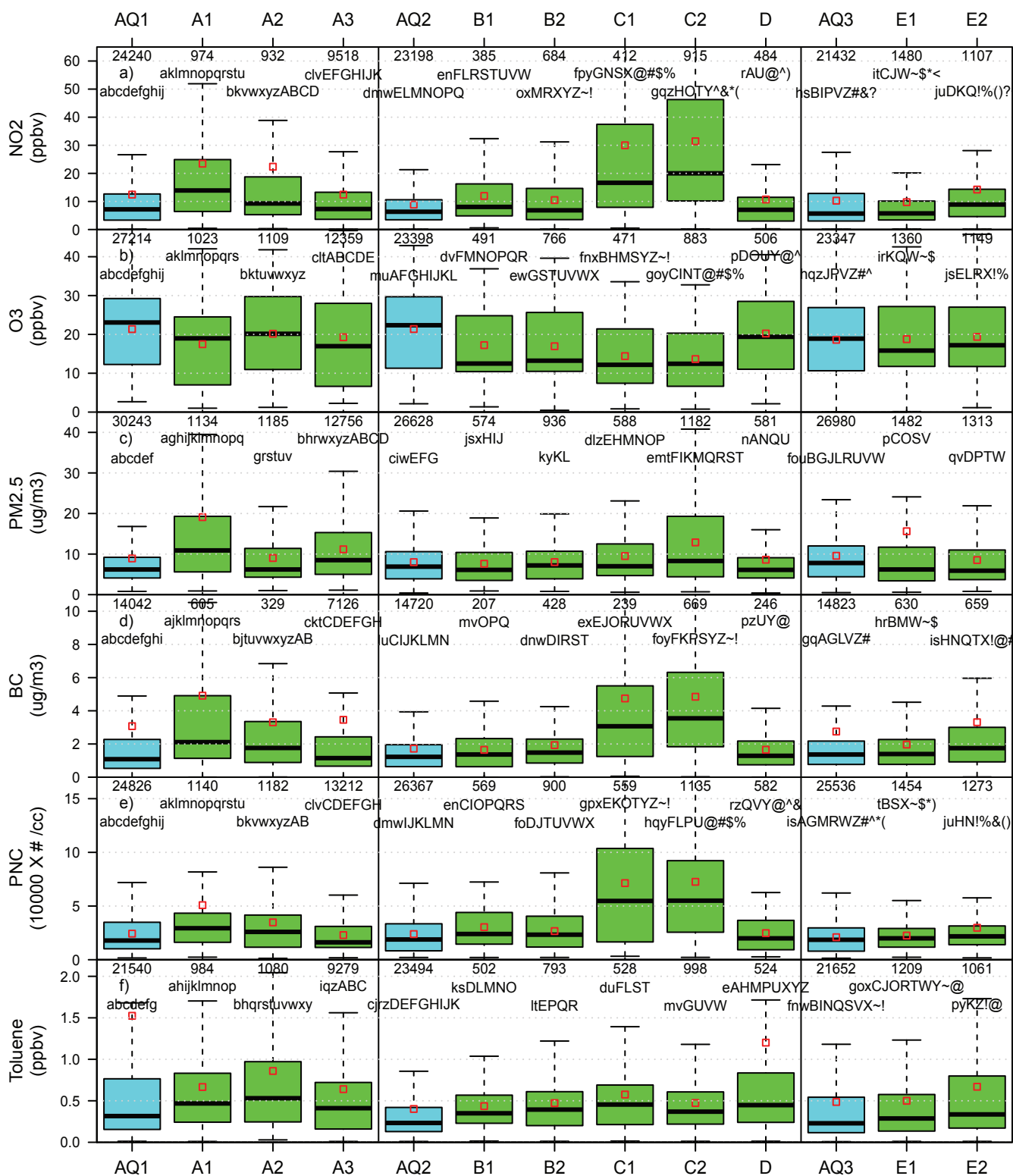


Fig. SM-A3: Same as Fig. 4 with the original 1 s data and letter categories identifying statistically significant differences. Pairs of location with matching letters are significantly different from one another (p -value < 0.05) according to the Wilcoxon Rank Sum test for pairwise group comparison.

B. Supplemental Table

Table SM-A1: Average values of several pollutants as calculated from the average of all measurements at distances between 1000-1500 m from the center of the Highway (background value, first row) and scale-up factors (i.e., percentages of increase relative to the background value) for each 50 m bin relative to the background (%). First bin (-20-20 m) includes measurements taken on the highway.

Distance (m)	NO ₂	NO	O ₃	PNC	PM _{2.5}	PM ₁₀	BC	CO	HOA
Background value:	7.1 (ppb)	5.3 (ppb)	18.2 (ppb)	24053 (#/cc)	6.8 (µg m ⁻³)	13.1 (µg m ⁻³)	1.0 (µg m ⁻³)	207 (ppb)	0.35 (µg m ⁻³)
-20 - 20	668	2353	44	392	200	284	342	231	306
20 - 70	273	792	70	95	91	135	271	137	256
70 - 120	285	377	88	88	101	92	238	202	220
120 - 170	218	173	117	95	106	92	238	161	197
170 - 220	265	144	124	103	106	76	170	161	220
220 - 270	268	120	115	111	88	102	105	141	160
270 - 320	225	168	96	108	120	124	165	132	160
320 - 370	208	335	79	102	95	110	178	160	160
370 - 420	169	207	78	102	98	65	128	153	160
420 - 470	147	146	82	126	97	89	120	114	160
470 - 520	136	124	119	123	88	83	119	115	160
520 - 570	153	131	103	108	91	71	102	107	160
570 - 620	132	114	118	98	95	68	137	105	152
620 - 670	111	114	119	74	97	89	93	90	152
670 - 720	108	126	119	74	91	86	41	91	125
720 - 770	106	82	121	83	92	118	71	91	125
770 - 820	107	101	119	94	98	89	92	85	125
820 - 870	122	124	119	98	98	79	100	95	120
870 - 920	109	105	120	90	95	86	95	88	102
920 - 970	118	208	120	94	106	99	107	105	102
970 - 1020	123	159	121	104	110	102	73	121	120

C. Description of the instrumentation inlets to CRUISER:

The inlets for the air quality instruments are located at the roof of the vehicle, ~3.6 m above ground, oriented near the front left side. There were two particle and two gas inlets. The PTRMS had its own ¼ inch Telfon inlet line with a Teflon filter outside at the entrance. The other gas analyzers utilized another separate Teflon line with splitting inside CRUISER as required for the different measurements. The main particle inlet draws air in at a 16.7 L min⁻¹ through a cyclone to achieve a 2.5 µm size cut followed by a 3.18 cm OD stainless steel sampling tube of 1.88 meters in length. Inside CRUISER this tube is surrounded by a 15.24 cm PVC pipe containing an external sheath air flow drawn from outside, which serves to keep the sample air containing particles at ambient temperature as long as possible to avoid condensation in summer and evaporation in winter. The AMS, CPC and PA are connected to the base of this 1.88 meter tube drawing air, approximately isokinetically, to their individual inlets through stainless steel (1/8-1/4") and flexible conductive tubing. The GRIMM Dustmonitor has its own ~1.8 meter stainless steel tube extending through the roof with the GRIMM multi-directional inlet drawing at 1.2 L min⁻¹. This separate inlet was needed to enable the capture of coarse particles (i.e., the main inlet has a cyclone), but due to its slow flow rate and the impact of horizontal speed on the capture efficiency of these large particles a correction based upon CRUISER's speed was required.

Hydrocarbon-like Organic Aerosols (HOA) mass contributions were obtained from the AMS using the positive matrix factorization (PMF) method (Paatero and Tapper, 1993), which interprets the measurements using factor analysis methods. A recent review of multivariate factor analysis techniques applied to AMS is presented in Zhang et al. (2011). AMS measurements were run through PMF using the toolkit available from: <http://tinyurl.com/PMF-guide>. HOA is expected to provide a unique measure of fine (PM₁) organic particle mass largely associated with motor vehicle exhaust (Canagaratna et al., 2010).

References:

Canagaratna, M. R., Onasch, T. B., Wood, E. C., Herndon, S. C., Jayne, J. T., Cross, E. S., Miake-Lye, R. C., Kolb, C. E. and Worsnop, D. R.: Evolution of vehicle exhaust

particles in the atmosphere, *Journal of the Air & Waste Management Association*, 60(10), 1192(12), 2010.

Paatero, P. and Tapper, U.: Analysis of different modes of factor analysis as least squares fit problems, *Chemometrics and Intelligent Laboratory Systems*, 18(2), 183–194, doi:10.1016/0169-7439(93)80055-M, 1993.

Zhang, Q., Jimenez, J. L., Canagaratna, M. R., Ulbrich, I. M., Ng, N. L., Worsnop, D. R. and Sun, Y.: Understanding atmospheric organic aerosols via factor analysis of aerosol mass spectrometry: a review, *Analytical and Bioanalytical Chemistry*, 401, 3045–3067, doi:10.1007/s00216-011-5355-y, 2011.

D. Speed correction for particulate matter (PM) measurements

Speed correction was applied to the particles measurements (PM_{10} , $PM_{2.5}$ and $PM_{1.0}$), to account for the effect of vehicle speed on collection efficiency of the inlet to the GRIMM dust monitor. A factor was estimated separately for each of the three particle size ranges by comparing PM values at the stop sites to the measurements during the approach to and leaving the stop site in a radius of 500 m around the site and within a timeframe of 30 min before and after the stopping period. This assumes that there is relative homogeneity in neighbourhood PM_{10} , $PM_{2.5}$ and $PM_{1.0}$ and that with a large number of pairwise comparisons of mobile to stationary mass measurement that if CRUISER speed impacted the mass measurement a trend in the ratio of stationary to mobile as a function of speed would be evident. Mobile measurements associated with $NO > 5$ ppb were removed as the corresponding PM_{10} , $PM_{2.5}$ and $PM_{1.0}$ might be influenced by a very local combustion source (i.e., nearby vehicles) and are not comparable with the recent neighbourhood concentrations determined when CRUISER was stationary. Similarly, measurements with zero speed were excluded to avoid impact from the mobile lab's own plume or other vehicle idling ahead of the lab in this analysis.

The ratio between the 'ambient' and the mobile measurements meeting the above criteria was calculated and a value of one was subtracted to derive the relative increase in PM according to the stationary measurement relative to the mobile measurement (i.e., $dPM = (\text{stationary PM/mobile PM}) - 1$). The relative increase values were then regressed against the vehicle's speed for each PM size where the slope of this relationship provides a speed-dependent correction factor. The robustness of the speed effect on the stationary to mobile measurement ratio and its magnitude was examined by separately analyzing 10,000 randomly selected subsets ($N=855$) of the CRUISER data. This approach assessed the sensitivity of the slope to what portion of the data were used, providing a measure of the confidence in the correction factor, as indicated by the variability in the slope among the 10,000 regressions.

Figure SM-D1 presents a sample scatterplot for each of the three particle sizes and Table SM-D1 gives the median correction factors, the standard deviations obtained among all 10,000 regressions. The red lines on the plots are a linear fit to this relationship and the slope provides a speed-dependent correction factor. The dashed blue lines are the 99% confidence limit of the predicted regression. As expected, as the speed approaches zero the magnitude of the relative increase or scale-up (ratio-1) becomes zero and as the speed

increases the scale-up increases. The slopes for the PM₁₀, PM_{2.5} and PM_{1.0} relationships increase with the upper size cut for the PM measure, which reflects the greater influence of air flow on the particles with larger mass and provides greater confidence that the pattern observed is related to the effect of speed on particle collection efficiency of the inlet.

Based upon the evidence of a zero intercept, a highly statistically significant positive slope among almost all 10,000 regressions, the small standard errors and a physically meaningful increase in slope with upper size cut we concluded that our approach provided a reliable measure of the effect of speed and that a speed-dependent correction of the PM measurements was important to utilize to insure that the mobile measurements are not biased low. This is expected to provide more appropriate comparisons of concentration between the size fractions, between the mobile and stationary measurements and among locations given that CRUISER speed was not constant.

After calculating the correction factors from the median of all 10,000 regressions they were then applied to all mobile measurements by the following formula:

Corrected PM = Original PM x (speed x CF + 1),

where the speed is measured in km h⁻¹ and CF is the correction factor. Note that the median slope among the 10,000 regressions and the slope obtained using all data points in a single regression were nearly identical.

The three graphs in Figure SM-D2 show the magnitude of the correction comparing the distribution of the uncorrected to the corrected PM measurements as a function of speed. For a majority of the mobile measurements reported in the paper the speed was 40 km h⁻¹ or less due to the types of roads the mobile lab spent the most time driving on. As can be seen, the correction does shift the distribution of PM mass and this shift is larger at higher speeds and for the PM measurements with the larger upper size cut. For PM_{1.0} the shift in the average mass is less than 1 µg/m³ up to 40 km h⁻¹, for PM_{2.5}, it is slightly above 2 µg/m³ and for PM₁₀ the shift is 15 µg/m³ at these speeds.

The measurements of PM₁₀ show that much larger values can occur due to resuspended dust; a small number of coarse particles can contribute considerable mass. As a result, greater spatial heterogeneity is expected in PM₁₀ and there will be larger scatter in the relationship between ambient and mobile observations and potentially less confidence in being able to make accurate corrections for each individual measurement. However, the

statistical significance of the slope (p-values <0.0001) suggests that mean PM10 values should be adjusted to more-accurately portray the average spatial patterns in mass. Figure SM-D2 further shows that the size of the increase in the mass due to the correction for PM10 is, on average, 15 $\mu\text{g}/\text{m}^3$ at speeds in the 30-40 km hr^{-1} range. This increases the average mass from about 20 $\mu\text{g}/\text{m}^3$ to about 35 $\mu\text{g}/\text{m}^3$. Thus, for PM₁₀, our analysis of how the speed of the vehicle and hence the speed of the air flow past the inlet to the GRIMM influenced the resulting mass measurement indicates that if this is not accounted for the values reported will be biased low and gradients in average concentrations may not be accurately represented.

The plots exhibiting the regressions undertaken to derive the corrections show there is considerable scatter in the relationship, which is due to neighbourhood scale heterogeneity in PM and noise in the 6 second GRIMM measurements. However, the relationships behave as expected (i.e., positive slope and equal range of scatter on both sides of the regression line), thus supporting our methodology and its assumptions, and indicate that correction, applied in a consistent fashion, is important to report more-reliable average concentrations and gradients from mobile measurements. Clearly more attention needs to be paid to this issue for mobile measurement studies exploring PM, especially if coarse particles are of interest. Interestingly, our results show that for measurements that use a slow inlet speed such as the GRIMM even the smaller particles (i.e., PM_{1.0}) are sensitive to the flow across the inlet induced by vehicle motion.

Table SM-D1: Mean and median slopes and standard deviation among the 10,000 independent regressions deriving GRIMM correction factors by particle cut size.

Particle size	Mean Slope (h km ⁻¹)	Median Slope (h km ⁻¹)	Standard Deviation (h km ⁻¹)
PM ₁₀	14.03x10 ⁻³	13.40x10 ⁻³	6.24x10 ⁻³
PM _{2.5}	6.74x10 ⁻³	6.53x10 ⁻³	2.47 x10 ⁻³
PM _{1.0}	3.59x10 ⁻³	3.52x10 ⁻³	1.23 x10 ⁻³

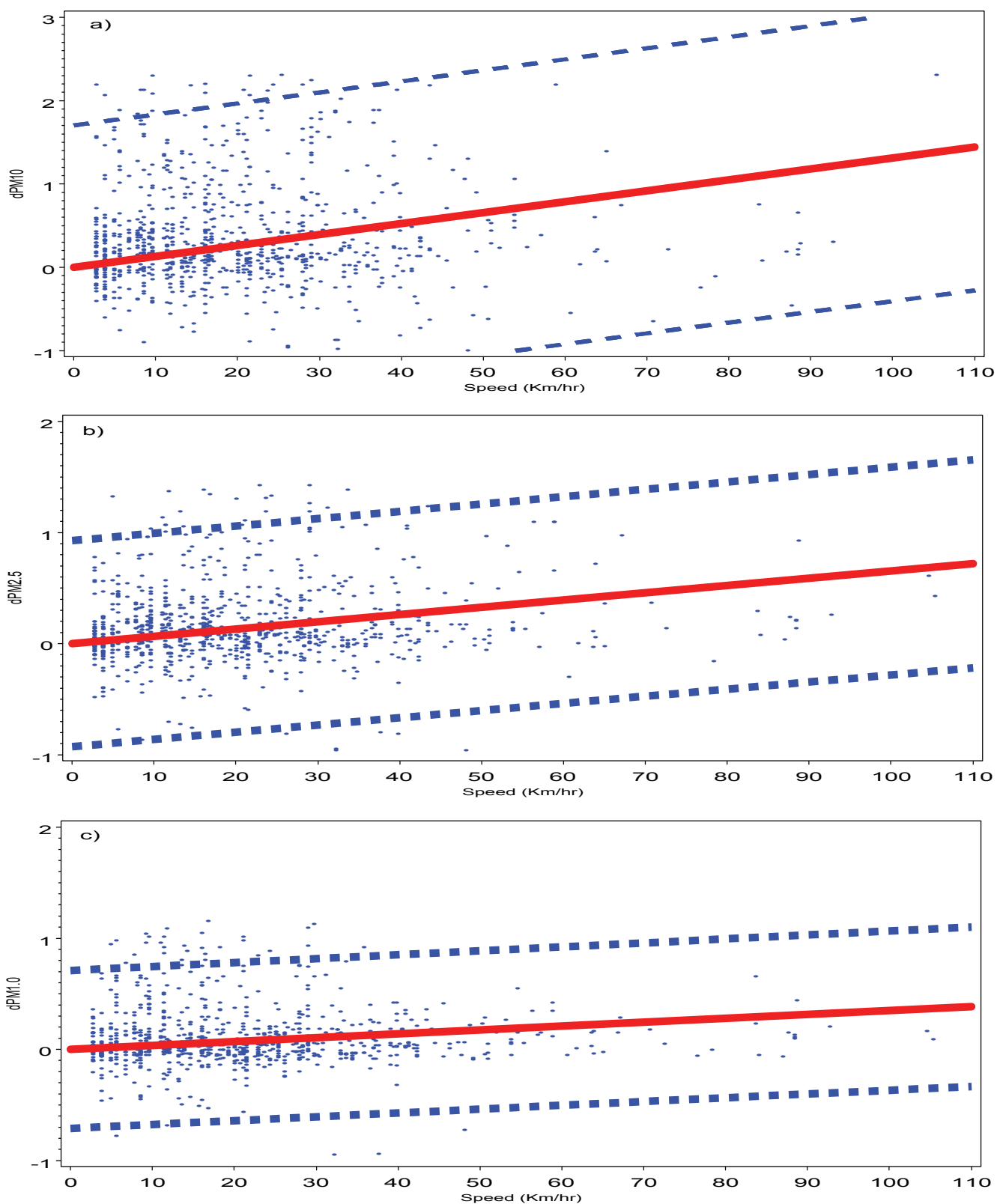


Fig. SM-D1: Scatterplots of the difference between the stationary and mobile measurements vs. vehicle speed for PM_{10} (a), $PM_{2.5}$ (b) and $PM_{1.0}$ (c)

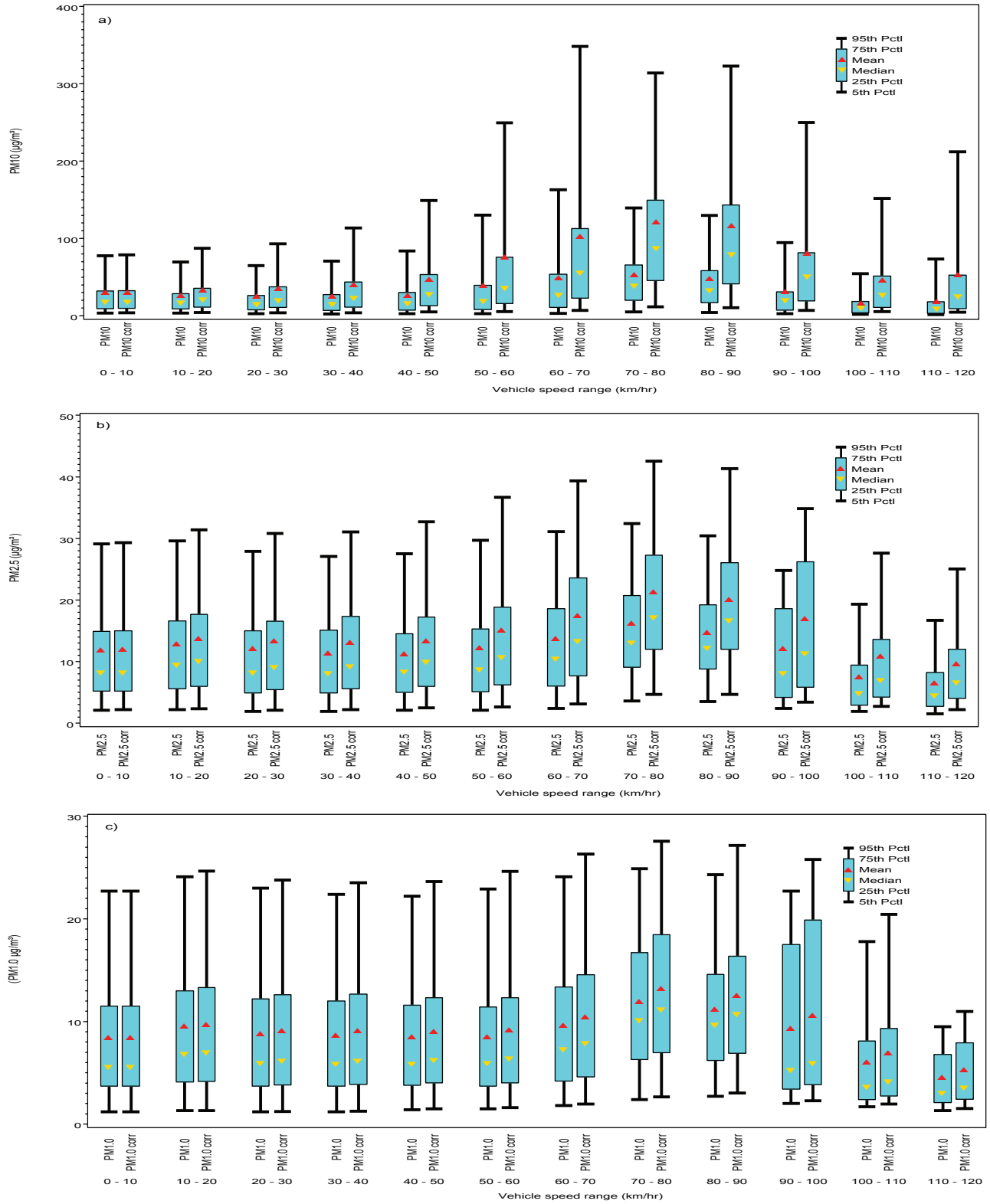


Fig. SM-D2: boxplots the corrected and uncorrected PM measurements for different ranges of vehicle speeds for PM₁₀ (a), PM_{2.5} (b) and PM_{1.0} (c)

E. Comparison of CRUISER's and VdM measurements

Instrumentation: Table 1 lists the instrumentation and methods used on CRUISER. Similar to CRUISER, VdM used Thermo Scientific instruments (Waltham, MA). However, for the routine VdM monitoring, trace level instruments were not used and calibrations were done over a larger range with less focus on low concentrations. Also, there were fewer zero readings compared to CRUISER (critical for low CO) and one minute VdM readings for PM_{2.5} were not possible (VdM used a Thermo Scientific Tapered Element Oscillating Microbalance with the Filter Dynamic Measurement System option to improve measurement of semivolatile material; FDMS-TEOM). In addition, one instrument was used by VdM for NO and NO_x with switching between measurement modes every 30 seconds, which can lead to incorrect NO₂ in areas impacted by frequent NO plumes. Furthermore, the converter used in the VdM instruments did not provide a specific measure of NO₂ (Lee et al., 2011) as was the case for CRUISER.

Comparison method: For direct comparison, CRUISER's one second measurements were first averaged to one minute values and the concurrent CRUISER and VdM one minute measurements during each 10-30 minute stop were then averaged. Only minutes with more than 45 one second measurements available (i.e., after excluding 1 s measurements due to probable impacts from CRUISER's own emissions) for both CRUISER and VdM were used to compute the stop period averages. There were six AQ sites with such paired measurements, although a full suite of pollutants were not monitored by VdM at each site. Also, due to the proximity of safe or accessible parking locations relative to the sites the actual distance between CRUISER and each site varied (~10-100 m; typically 20 m). In addition, for one site (AQ4) there was a large difference in sampling height since the VdM measurements were from a rooftop of a few stories.

Results: Given the differences in the instruments, how they were operated, the short time for each comparison (typically ≤15 minutes of paired readings per point) and the distance between inlets, reasonable agreement was found for the available pollutants. Figure SM-E1 shows scatter plots of CRUISER vs. VdM measurements during times when CRUISER was parked near the AQ sites. For NO, NO₂, NO_x, CO, O₃, PM_{2.5} and SO₂ the R² values are 0.83, 0.62, 0.85, 0.37, 0.81, 0.60 and 0.16, respectively, and the slopes (CRUISER/AQ) are 0.94, 0.72, 0.78, 0.93, 0.88, 0.66 and 0.77, respectively. For SO₂

(Fig. SM-E1d), we have excluded one high point associated with a local plume ($\text{SO}_2=34$ ppbv) that occurred during a stop because it was highly influential on the regression results and obscured the relationship at the more typical lower concentrations. When this point is included the R^2 is large (0.96) and the slope increases to 1.07 thus indicating better agreement over the larger range of concentrations possible. For CO there are a limited number of points for comparison due to few VdM sites with data. There were also considerable differences in the operation of the instruments and thus, a low correlation is not surprising. The fact that considerably more of the VdM CO values in Fig. SM-E1a are less than typical regional background levels suggests that for the low concentrations occurring in Montreal the CRUISER method was producing more accurate results. Similarly for $\text{PM}_{2.5}$ (Fig. SM-E1c), the measurement methods were significantly different and VdM only reported hourly values. There are good correlations for NO, NO_2 and NO_x . For NO_2 and NO_x VdM concentrations tended to be higher than CRUISER at the higher concentrations with a larger discrepancy for NO_2 , which is likely due to the non-specific measure of NO_2 utilized by VdM.

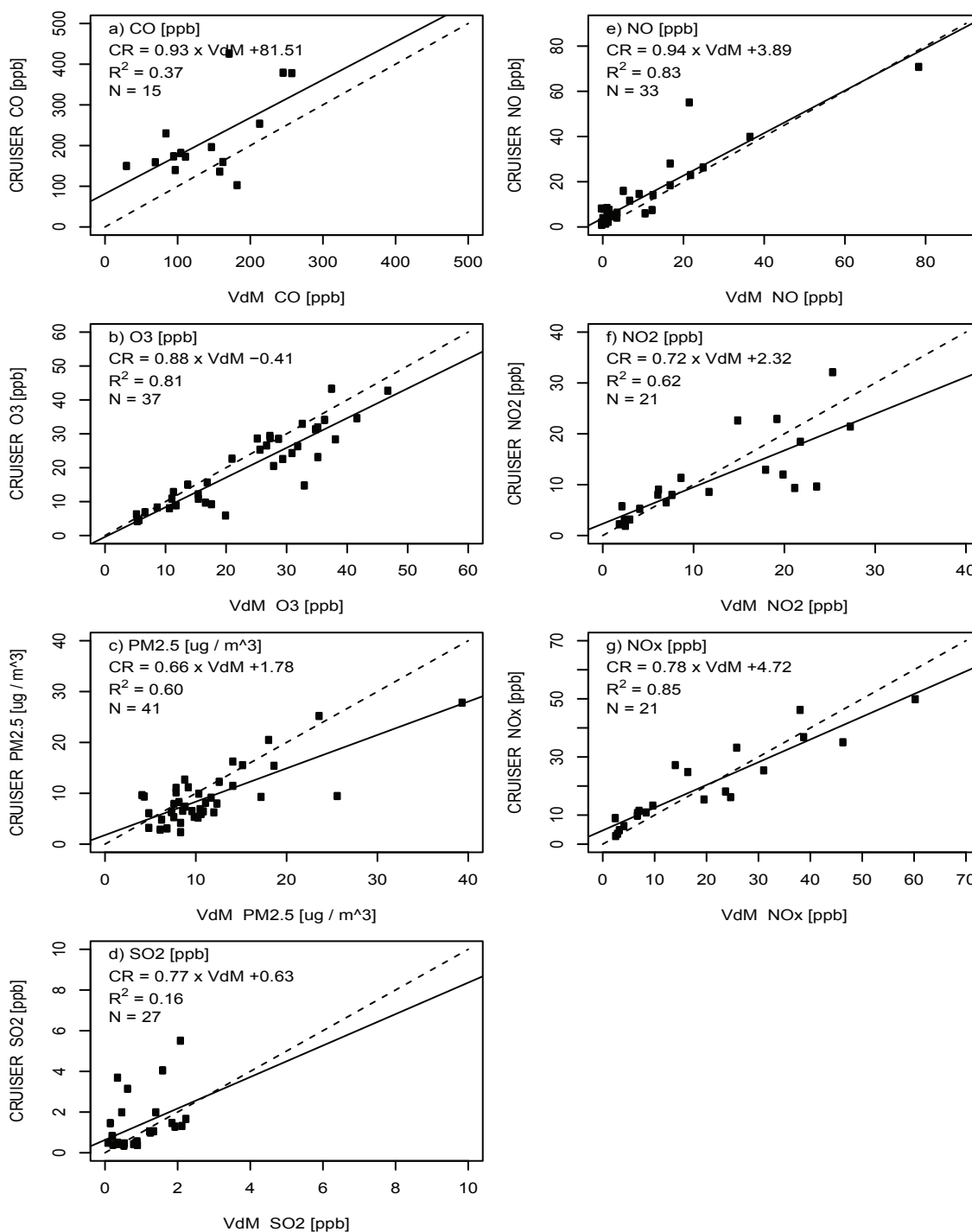


Fig. SM-E1: Scatter plots of CRUISER's vs. VdM AQ sites measurements during times CRUISER was parked in close proximity to AQ sites.

References:

Lee, C. J., Brook, J. R., Evans, G. J., Martin, R. V. and Mihele, C.: Novel application of satellite and in-situ measurements to map surface-level NO₂ in the Great Lakes region, *Atmos Chem Phys*, 11(22), 11761–11775, doi:10.5194/acp-11-11761-2011, 2011.